This article has been accepted for publication in IEEE Transactions on Haptics. This is the author's version which has not been fully edited and content may change prior to final publication. Citation information: DOI 10.1109/TOH.2023.3273908

A Soft Hand Exoskeleton with a Novel Tendon Layout to Improve Stable Wearing in Grasping Assistance

Tommaso Bagneschi[1], Domenico Chiaradia[1], Gabriele Righi[2], Giulio Del Popolo[2], Antonio Frisoli[1], Daniele Leonardis[1]

***Abstract*— We present a novel soft exoskeleton providing active support for hand closing and opening. The main novelty is a different tendon routing, folded laterally on both sides of the hand, and adding clenching forces when the exoskeleton is activated. It improves the stability of the glove, diminishing slippage and detachment of tendons from the hand palm toward the grasping workspace. The clenching effect is released when the hand is relaxed, thus enhancing the user's comfort. The alternative routing allowed embedding a single actuator on the hand dorsum, resulting more compact with no remote cable transmission. Enhanced adaptation to the hand is introduced by the modular design of the soft polymer open rings. FEM simulations were performed to understand the interaction between soft modules and fingers. Different experiments assessed the desired effect of the proposed routing in terms of stability and deformation of the glove, evaluated the inter-finger compliance for non-cylindrical grasping, and characterized the output grasping force. Experiments with subjects explored the grasping performance of the soft exoskeleton with different hand sizes. A preliminary evaluation with Spinal Cord Injury patients was useful to highlight the strengths and limitations of the device when applied to the target scenario.**

Fig. 1: Preliminary prototype of the compact soft exoskeleton. Actuator and tendon transmission are arranged around the palm and hand dorsum, with no remote mechanical parts.

I. INTRODUCTION

The role of the hand is crucial in our physical interaction with the environment: most of the Activities of Daily Living (ADL) involve the use of the hand for fine manipulation, grasping, and the use of tools. Restoration of hand motor functions is then fundamental for patients who have completely or partially lost their motor abilities to gain a better quality of life. Robotic devices supporting the hand can play an important role both for assistance purposes [1], [2] and for neurorehabilitation, where haptic feedback, congruent with motor intention, can promote and guide brain plasticity toward a more normal restoration of motor functions [3].

To convey motor assistance at the level of the hand is a challenging objective in the design of robotic devices, due to the complexity of the hand kinematics, variability of hand sizes, limited available workspace, and relatively high forces involved. Different approaches have been proposed in the literature [4], including rigid exoskeletons, underactuated solutions to better adapt to the user's hand, and soft exoskeletons and gloves with tendon-driven or pneumatic actuation.

Rigid exoskeletons are capable of exerting higher and more precise forces at the different contact points, yet they suffer a lack of adaptation to different hand sizes, with consequent misalignment of joints for the hand kinematics. This is likely to prevent the comfortable wearing of the device, compromising its usability [5]. Underactuated self-aligning kinematic design [6] and intrinsically adaptive rigid kinematic solutions have been proposed, the latter incorporating the finger itself in a parallel kinematic arrangement [7]. These solutions improve adaptability to different hand sizes, although it becomes more critical for a stable and rigid fixing of the exoskeleton's links to the finger phalanxes, in order to guarantee the desired transmission of forces [8].

The introduction of soft materials in robotics fostered the development of novel hand exoskeleton devices with improved adaptability, comfort in wearing, and lightweight structure [9]. The soft exoskeleton approach exploits the rigid kinematic of the finger itself, by only adding an external actuation system

Pneumatic actuated soft gloves implement inflatable chambers, usually placed on the finger dorsum, to assist hand closing [10], [11] or hand opening as in the case of the AirExGlove [12] intended for post-stroke patients with muscle spasticity. A further step toward compactness and adaptability is presented in [13], with a modular fishbone structure. Also, the pneumatic soft exoskeleton glove presented in [14] proposes an extremely light Mc Kibben-based antagonistic pairs of muscles similar to the human anatomy. Despite the lightweight of parts applied to the hand, the need for remote air pumps and a pressure modulation system makes these

[1] are with the Institute of Mechanical Intelligence and the Department of Excellence in Robotics & AI, Sant'Anna School of Advanced Studies, Pisa, Italy name.surname@santannapisa.it

[2]are with the Spinal Unit, Careggi University Hospital, Firenze, Italy name.surname@aou-careggi.toscana.it

systems relatively complex.

A hybrid approach combining the properties of rigid link structures and soft mechanisms was presented in work [15] and similarly, in [16]. Butzer [15] uses flexible semi-rigid elements and combines them to form a layered spring mechanism that assists in opening and closing the hand.

A more compact solution makes use of cable transmission, mimicking the biological arrangement of muscle tendons. The method has been widely explored in literature, resulting in soft and slim gloves actuated by conventional electromagnetic motors [17], [18], [19], [20], [21].

Due to the geometry of the finger and the tendon placement, in order to exert a certain force at the fingertip, the tendon has to be pulled with a considerably higher loading force [17]. The problem then is how to effectively guide the tendon through the soft structure of the glove: anchor points and sheaths have to be stable during operation, but the excessive tightening of belts, rings, or other supports to the hand has to be prevented to avoid discomfort and other undesired effects.

The design proposed in [19], [22] introduces an interesting solution with open ring supports around the finger and two parallel pulling tendons: it allows to tighten of the soft supports around fingers only when the tendon transmission is loaded.

Regarding the actuators, proposed designs of tendon-driven hand exoskeletons place the motors remotely with respect to the hand, through Bowden cables [6], [17], [18], [19], [23]. On one side this choice reduces weight and encumbrance at the hand, on the other side it requires longer Bowden cables, relatively flexible, that compromise the overall wearability of the system and efficiency of the transmission. Moreover, depending on how the insertion point of the Bowden cable is fixed to the hand, (usually in proximity to the wrist), rotation of the wrist can affect the actuation of the fingers. An interesting prototype where the actuators are located on the dorsal part of the hand is presented in [24]. We desired to further develop this approach, in terms of better distribution of the pulling forces, comfort, and adaptation to the user's hand.

In addition, another very important challenge is the wearability and comfort of the system. Patients have limited motor control of the impaired hand, and this imposes significant difficulties in donning glove-like wearable devices. Outside the robotic field, passive rehabilitation gloves have usually an open structure, i.e. with thimble modules connected by an elastic dorsal structure (rehabilitation gloves by Saebo Inc.), allowing separated finger donning. For the donning procedure, surprisingly soft, more comfortable exoskeletons are more challenging to design with open and detachable modules with respect i.e. to rigid exoskeletons.

In rigid exoskeletons, links are usually located at the hand dorsum, and finger modules can be fixed one by one to fingers through fabric bands. Soft exoskeletons instead have cable routing and transmissions at both sides of the fingers, making it harder to obtain a truly open, accessible structure for finger donning. Moreover, tendons are tightly routed through sheaths and guiding rings, impeding the implementation of detachable modules with interrupted tendon transmission (the tendon connection point should then pass through the sheaths). Still, certain design choices can improve wearability and donning procedures also in soft exoskeletons design, obtaining partially open structure at least for finger modules after the metacarpal segment [19], [25].

In this work, we present a novel soft hand exoskeleton aiming at stability and comfort in the user's hand. The proposed design implements a novel arrangement of the tendon routing with an actuator embedded at the hand dorsum: tendons are folded around both sides of the hand, providing a more stable wearing of the device and a more balanced distribution of the pulling forces between the thumb and the other fingers during the hand closure. This is expected to improve also comfort since clenching forces are applied only when grasping is active. The modular soft 3D printed finger units, inspired by [19] with the open ring structure, improve the adaptability of the device to different hand sizes, wearability, and donning for motor-impaired subjects.

In the study, we present the design, development, and experimental characterization of the prototype. The first experimental part is dedicated to the finger modules, with FEM simulations and experimental loading tests measuring structural robustness, lateral compliance for different finger sizes, and interface pressure between the ring and the finger skin for the comfort of the user.

The second experimental part measures the effect of the proposed routing on the overall glove deformation using optical markers and a comparative conventional routing arranged on the same prototype. Then, inter-finger compliance for non-cylindrical graspings is characterized, and the final output of grasping assistance is measured in a group of six subjects. Finally, a preliminary evaluation of the prototype with two SCI patients evidences the strengths and limitations of the developed solution.

II. METHODS

A. Soft Exoskeleton Design and Implementation

The developed hand exoskeleton aims at supporting hand grasping through a compliant soft structure: it implements one actuator (one degree of freedom or 1-DoF) for active assistance of both hand closing and opening and proposes a novel tendon routing to improve stability when grasping is assisted. The design has been further developed from a preliminary concept presented in [25] that implemented a simplified structure and transmission with a passive opening of the hand. The prototype actuates three fingers: thumb, index, and middle finger. This choice allowed testing the proposed approach with reduced complexity of the whole device.

1) Modular Finger Units: Finger units consist of a series of Thermoplastic Polyurethane (TPU, shore hardness 95A) open rings and a thimble. They are designed to be printable in flexible filaments with the conventional Fused Deposition

Modeling (FDM) 3D printing method. Polytetrafluoroethylene (PTFE) tubes are embedded at the tips and in the middle part of the open rings where tendons are routed. The number of rings can be varied in number and dimensions to better fit phalanges of different lengths and sizes. Screw terminals on the thimble allow to release of the tendons and to change rings without re-routing the transmission of the whole device.

The open ring approach uses two parallel flexion tendons per finger, as presented in [19], [22], and two parallel extension tendons. The design solution has been chosen due to its improved stability and comfort in wearing. The open structure allows to relax clenching forces when the transmission is unloaded. The kinematic model of the soft open ring modules is shown in [19]. Concerning the referenced work, we introduced a redundant number of rings to better adapt to different lengths of the fingers. Also, fabrication in 3D printing, rather than using flat silicone foils, allows for a more precise fit of the rings when tendons are relaxed.

2) Tendon Routing and Actuation : The proposed tendon routing aims at improving the stability of the device when activated, by exerting pressing forces on the palm plate. To this aim, transmission branches are separated at the palm and folded around the hand sides, as shown in figure 2. Concerning the conventional design with tendon insertion points at the palm, it adds force components between the palm plate and the dorsum plate, that are expected to increase the stability of the device when tendons are pulled. On the other side, to allow a more comfortable wearing of the device when actuators are not active. The desired effect is also an advantage for grasping since it keeps the palm plate and tendons closer to the hand and out of the grasping workspace.

The obtained tendon layout allows also for embedding the actuator directly at the hand dorsum, although it would work also with remote actuators and Bowden cables. In the presented prototype we explored the embedded actuator solution: the advantage is a compact device with no remote mechanical parts and just a flexible electric wire for electronics and batteries that can be placed at the forearm or arm segment. Conversely, Bowden cables, one for each tendon, should be routed from the hand to a remote location, possibly impeding movements due to the relatively stiff sheaths. The disadvantage is a more cumbersome device at the hand. The total mass of the prototype was $124 \pm 1\ g$ (including the actuator, and excluding the remote battery or power supply). The dimensions of the actuator module at the hand dorsum were $76.8 \times 60.1 \times 25.5 \times\ mm$.

To this purpose the routing of the closing transmission has been modified with respect to conventional designs: two different branches, one grouping the index and middle finger, the other for the thumb (plus ring and little finger in further prototypes) are routed laterally around the hand palm to reach the hand dorsum (Figure 2).

Transmission branches are grouped at the hand dorsum by a single actuation pulley with multiple grooves. The pulley accommodates also the extension branches: in this way, both directions of actuation are implemented with a single motor. The total number of grooves is 6, with 3 dedicated to extension and the remaining 3 to flexion. Each groove is capable of accommodating a pair of cables coming from a finger unit.

The required stroke length of the tendons for accomplishing a full range open-closing movement of the finger was measured for a medium hand size (length: $184\ mm$). For each finger (thumb, index, and middle fingers), these stroke lengths were empirically measured with the device worn at the hand and actively moved by the subject from the open to close hand pose. Then the diameter of each pulley groove (two per finger, for extension and flexion cables) was calculated proportionally to each stroke length. These diameters are shown in Table I. In case the pulley is not customized for the specific user, the error introduced in the kinematics is limited to different proportions between finger lengths, and not by the overall hand size scaling (compensated by just a different number of turns of the whole multi-groove pulley). In case of slack-tendon, other design introduced a dedicated mechanism for avoiding derailing, as in [19]. In our case we had more strict dimensional constraints due to the actuators embedded at the hand-dorsum. We then improved robustness to slack-tendons by increasing the height of the grooves in the pulley up to the dimensional limits of the actuator volume. This solution proved robust also in the extreme experimental condition of the inter-finger compliance presented in Section II C (i.e. one finger is blocked by stiff obstacles while other fingers are closed by the actuator). Details of the actuation unit is shown in Figure 3. The actuator (Lynxmotion Smart Servo Motor ST1) is a gear-reduced DC motor with embedded drive electronics and position sensor ($12\,V$ nominal voltage, $1.37\,Nm$ maximum static torque, $360\,°/s$ maximum speed). The stiffness of the tendon wire was measured and equal to $0.15\ N/mm$ for meter. This value has to be scaled to the lengths of the different transmission branches depending on the finger and on the subject hand size. As a reference value, the length of the transmission branch of the index finger in the open position was around $20\,cm$.

The soft exoskeleton structure is based on an elastic fabric glove reinforced by two rigid plates (3D printed in ABS) for the hand dorsum and palm, used to guide the PTFE tendon sheaths. The dorsum plate holds the actuator and the multi-groove pulley. Regarding the palm plate, the choice of ergonomic but more rigid support was taken after the prototype iteration [25] with a similar part printed in TPU. The increased stiffness allows for keeping the plate more adherent to the palm when the exoskeleton is activated, thus improving grasping capabilities.

A flexible TPU wristband was added to hold the exoskeleton more firmly, especially when the device is activated in the opening direction. In the closing direction, the peculiar tendon routing allows a stable and balanced wearing of the device. To improve donning of the device for impaired hands, one side of the glove can be opened up to the fingers level by a zip closure.

This article has been accepted for publication in IEEE Transactions on Haptics. This is the author's version which has not been fully edited and content may change prior to final publication. Citation information: DOI 10.1109/TOH.2023.3273908

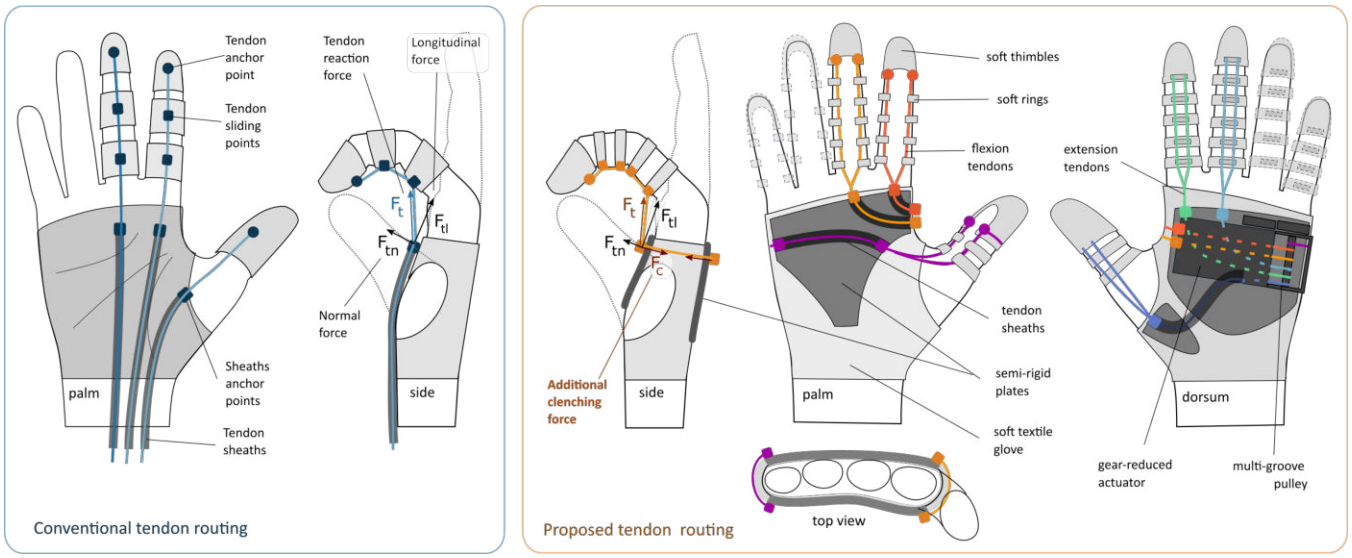

Fig. 2: Comparison of the conventional tendon routing with the proposed one: the latter adds a clenching force component around the hand palm, better-balancing reaction forces applied by tendons at sheath insertion points, and reducing the consequent deformation of the glove.

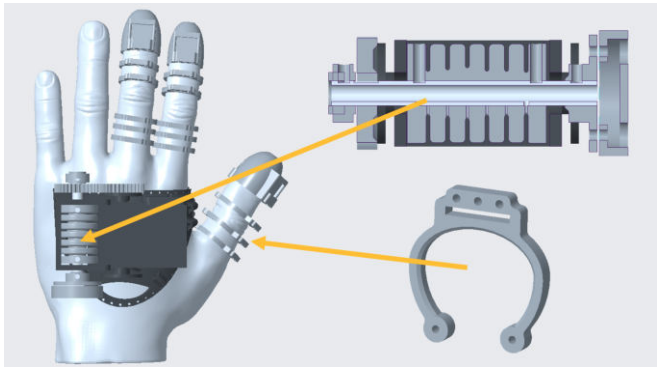

Fig. 3: CAD assembly of the components of the prototype. Highlighted the pulley of the actuation unit and an open ring.

	Thumb	Index	Middle
D extension $[mm]$	9	9.5	10.5
D flexion $[mm]$	10.5	11.2	12.2

TABLE I: Diameters of each groove of the pulley

B. Finite element analysis and mechanical characterization of the open rings

Two FEMs models were generated to simulate first the behavior of the 3D-printed open ring structure and second the interaction between the ring and the finger during the cable traction. The first model represents the traction and elongation of a TPU ring (internal maximum diameter of $19\ mm$, radial thickness $1.6\ mm$, axial thickness $3\ mm$). The magnitude of the traction force was decided based on the previous characterization of the servomotor. The actuator, powered at $9V$ and with a pulley of radius $10mm$, generates a traction force of $25\,N$. The force exerted on a single finger is one-third of the total force, so cautiously a force of $10\,N$ was chosen to test the ring traction. The elastic modulus for TPU was set at $26\,MPa$ from the datasheet.

The second model represents a phalanx and the ring, to which the traction force of the cables is applied. The following assumptions were made to simplify the model, while still keeping it reliable. The model considered is the case of the first ring on the proximal phalanx, that is, the ring on which most of the force is applied (figure 5a). The model was designed following the anatomy of the proximal phalanx [26]. Since the applied forces are low, the materials were considered isotropic with an elastic modulus of $70\,kPa$ for the finger soft tissue [27] and $11.5\,GPa$ for the bone [28]. Only flexion was considered for this model, as it is the loading condition that stresses the device and the hand the most. The sheaths, in which the cables run through the rings, were considered with zero friction: the assumption results in loading force components applied by the single tendon to the ring only in the transversal plane (the x-y plane in Figure 5). The forces F1 and F2 applied in space, as shown in figure 5d, would have a modulus of $4.16\,N$.

The open ring elements are conceived to be easily deformed in the lateral direction for compliance with different finger diameters. Instead in the vertical direction, they have to withstand the higher forces applied by the tendon transmission. An experimental setup was developed to test the mechanical properties of the open-ring elements. The same LSS ST1 servomotor and a force sensor (Futek LSB200) were placed at a fixed distance on two rigid supports and connected by two tendons to a sample TPU ring (internal maximum diameter of $19\ mm$, radial thickness $1.6\ mm$, axial thickness $3\,mm$). Experiments were performed in two different loading configurations, longitudinal and lateral, as shown in Figure 4. A slow ramp signal was provided to the actuator, measuring cable displacement, loading and unloading forces.

This article has been accepted for publication in IEEE Transactions on Haptics. This is the author's version which has not been fully edited and content may change prior to final publication. Citation information: DOI 10.1109/TOH.2023.3273908

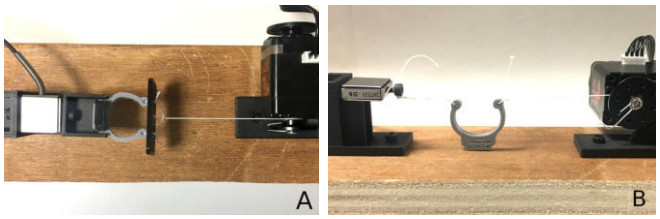

Fig. 4: Setup for the mechanical characterization of the open ring: a) ring longitudinal configuration; b) ring lateral configuration.

C. Experimental evaluation of wearing stability

An experiment was conducted to evaluate the improvements of the proposed transmission in terms of the stability of the glove when activated. Two different tendon routing layouts have been prepared and experimented with: a cable routing (R1) resembling a conventional layout presented in the literature (i.e. [19], [22], [24], and the cable routing (R2) proposed in this work. The mannequin hand model by Gyrobot [29] was taken as a mannequin hand to perform this test. The use of a mannequin ensured the repeatability of the test and avoided any possible compensation movement or muscular contraction involuntary introduced by subjects. For simplicity of the dual setup and the multiple tendon insertion points, the exoskeleton configuration for this specific experiment involved two fingers only: the thumb and the middle finger (Figure 2, image on the right). Additional sheath insertion points have been fixed at the palm plate, together with dedicated finger modules for the thumb and middle finger, interchangeable for the two experimental conditions. For the conventional routing, the servomotor was detached from the dorsum plate, fixed to a remote rigid base, and connected to the dedicated tendons.

Passive optical markers were placed on the mannequin and the OptiTrack V120 Trio was used to capture the movements of the actuated prosthetic hand. One marker was placed at the base frame, as a fixed reference, one at the palm plate, and one at the index fingertip.

The servomotor was actuated in the closing direction in an open loop, with three reference voltage levels corresponding to 50%, 75%, and 100% of the nominal supply voltage. The voltages were applied as square waves over 10 repetitions.

A second experiment was conducted, aimed at measuring inter-finger compliance given the 1-DoF actuation of the exoskeleton, using a single output shaft for all the routed tendons. In the absence of compliance between fingers, this might generate issues when non-cylindrical objects are grasped, due to force distribution and loosening of branches of the tendon transmission. In the experimental setup, we desired to generalize such conditions by introducing a rigid obstacle for one finger only and leaving the other free to close.

Passive optical markers were placed on the index and middle fingertips to track fingertip positions. A force sensor (OptoForce 3D force sensor OMD-10-SA-10) was mounted on a horizontal bar, colliding with the fingertip of the middle finger only. The servomotor was actuated in an open loop to pull in the closing direction, using two reference voltage levels, corresponding to the 25% and 50% of the nominal voltage. As for the previous experiment, references were applied as square waves over 10 repetitions.

A third experiment was conducted, aimed at measuring the pressure exerted over the hand palm during the actuation of the glove. Two Force Sensitive Resistor (FSR) sensors (FlexiForce™ A401 Sensor, Tekscan, Inc) were placed in two places in the palm, one under the index finger and one under the little finger, to better cover the surface of the semi-rigid palm plate in contact with the hand. These sensors (diameter 25 mm) are flat enough to be placed between the user's hand and the plates of the exoskeleton and were the most viable solution to measure the exerted pressure at the interface.

Three different supply voltage levels were applied in closing direction to the servomotor as in the first experiment and the three corresponding pressure levels were measured. This experiment was conducted on a healthy hand, because the mannequin hand was too stiff and would not have a perfect adherence on the plate.

D. Experimental evaluation with subjects

The prototype has been then evaluated in terms of output grasping strength and transmission efficiency (output fingertip force vs. actuator force) with subjects having different hand sizes. Finally, a preliminary test has been performed with two SCI patients to evaluate the effectiveness as an assisting device. The experimental procedures were approved by the Ethical Review Board of Scuola Superiore Sant'Anna (approval number 152021). The preliminary evaluation of the two SCI patients was carried out at the Spinal Unit, Careggi Hospital of Florence, Italy.

Six healthy subjects (aged 24-35, male) were enrolled: dimensions of the participants' hands are reported in Table II. The hand length was measured from the center of the wrist to the tip of the middle finger, the middle finger length from the fingertip to its base, and the hand width from the two lateral ends of the palm. They were asked to wear the exoskeleton and to extend their fingers, then the length of cables was adjusted using screw terminals at the thimble and the external flange of the actuation shaft. Subjects were asked to keep their hand relaxed during all the experimental sessions.

To estimate the grasping assistance of the developed prototype two sensorized objects have been introduced, similarly to [7]. One object estimates the grasping pressure for the exoskeleton-assisted hand: a pressure sensor (Bosch BMP280 pressure sensor) was placed under the bottlecap of a plastic water bottle. The bottle was filled with water to increase its stiffness. The second object measures the grasping force: it consists of a rigid handle divided into two halves, separated by a single-axis force sensor (Futek LSB200 force sensor).

Starting from a finger position in bare contact with the force-sensorized object, the first test increased motor torque linearly over time in the closing direction. The sequence

was repeated ten times. The servo motor was driven in an open loop (voltage reference) during the closing phase. Once the maximum output torque was reached, the actuator was driven back to the initial position in a closed loop. The voltage-torque characteristic of the actuator for quasi-static conditions was experimentally measured before the experiment (with the Futek LSB200 force sensor) and used to estimate the cable-pulling force in the presented results.

In the second experimental test, the exoskeleton was controlled in position (PID controller) starting from an open pose of the hand. The output command of the controller was saturated to reach, without exceeding, the maximum torque in static conditions, when i.e. the fingers got in contact with the grasped object. A sequence of ten full-range open-closing movements was executed by each subject with the pressure-sensorized object and ten with the force-sensorized object.

	S1	S2	S3	S4	S5	S6
Hand Length $[mm]$	183	184	173	200	180	196
Middle Fing. Length $[mm]$	80	78	79	88	80	86
Hand Width $[mm]$	85	88	85	86	86	93

TABLE II: Hand size data of each subject

E. Preliminary evaluation with SCI patients

A physiotherapist assisted in the wearing of the device. The first patient (44-year-old, female, with AIS A C7 tetraplegia) had a relatively small hand (hand length $15\ cm$) with medium spasticity and limited range of movement, given by tenodesis surgery, to use wrist tendons as a means of restraint of the finger joint, replacing natural ligaments. The patient was able to wear the exoskeleton with a semi-closed hand configuration. From this position, the thickness of the ring modules prevented further hand closure. Instead, the active opening was avoided in agreement with the physicians so as not to interfere with the patient's tenodesis. This prevented a proper grasping test.

The second patient (23-year-old, male, with AIS A C7 tetraplegia) presented a flaccid hand with medium-large hand size (length $20\ cm$). He was able to wear the exoskeleton, but the size of the elastic fabric glove resulted too tight and difficult to wear, despite the presence of the lateral zipper closing. The finger structure with open-ring elements instead, easily adapted to the different finger sizes.

In contrast to the first patient, the first test with no grasping objects was performed with the second patient, to verify that the exoskeleton could mobilize the hand. The exoskeleton was able to move the passive fingers in both closing and opening directions. Then, grasping of the pressure-sensorized object was performed with and without the assistance of the exoskeleton.

III. Results

The first FEM simulation showed that the TPU open ring structure, under the action of the overestimated load, reaches a maximum equivalent (von-Mises) stress of $4.6\ MPa$ and does not reach either break or yield points for the TPU (tensile stress at yield: $8.6\ MPa$, tensile stress at break: $39.0\ MPa$). The second FEM simulation shows the desired ring clenching around the finger. The equivalent stress on the ring remains contained and the soft tissue flattens against the bone where it unloads all stresses (Figure 5b and Figure 5c). Figure 5e shows how, on top of the finger, the contact is maintained (red surfaces), a portion of the ring slips (orange surfaces) and near the ring-finger interface a small portion of the finger surface deforms (yellow surfaces). Moreover, Figure 5f shows the pressure distribution on the skin of the phalanx which has a maximum value below $0.15\ MPa$. Since the human pressure-pain thresholds on fingers can be considered above $0.4\ MPa$ [30], the pressure calculated by the simulation can be considered acceptable and well below the threshold.

The mechanical characterization of the open ring elements highlighted, as desired, different mechanical behaviors in the two configurations. The force-displacement curve (Figure 6) for the longitudinal configuration shows higher stiffness than the force-displacement curve for the lateral configuration. In the second case the highly non-linear loading curve is due to the significant change in the geometry of the ring for high deformation: however, a lateral deformation (corresponding to the adaptation to different finger diameters), higher than $20\ mm$, is not expected.

From the first test with the mannequin hand, the two routing layouts have been compared by observing the displacement of the marker on the palm plate. Figures 7a, b, and c show tangent components to the palm of this displacement at different voltage references. At the same voltage applied to the servomotor, the y-axis displacement for the conventional routing is higher than that of the proposed routing. The first routing showed a y-axis displacement of $2\ mm$ to $-5\ mm$, against a displacement of $1\ mm$ to $2\ mm$ for the second routing. For the normal component of the displacement, Figure7d, e, and f show how the effects on the displacement are not only smaller but also opposite in sign, which means that the proposed routing tightens the glove on the subject's hand ($0.5\ mm$ to $1.5\ mm$ against $-1\ mm$ to $-0.5\ mm$). For each level of supply voltage, we compared the palm displacement distributions for the two conditions - routing 1 (R1) and routing 2 (R2). We checked the normality of the distribution using a Shapiro-Wilk test (significance level $\alpha = 0.05$) and we obtained that all data were normally distributed. Thus the statistical significance between R1 and R2 conditions was assessed with a paired t-test ($\alpha = 0.05$). All the differences were statistically significant with a p-value less than 0.001.

The second test with the mannequin hand showed a pronounced flexion of the index, while the middle finger was in contact with the OptoForce sensor fixed at the horizontal bar. At the 50% of the supplied voltage, the middle finger generated a force of $2.5\ N$. In this test, the displacement of the two fingers was calculated as the Euclidean distance from the position data in the 3D space of the finger markers with respect to the marker on the rigid frame. The index finger reached a maximum displacement of around $80\ mm$, while the middle reach the bar and stopped with a displacement of

This article has been accepted for publication in IEEE Transactions on Haptics. This is the author's version which has not been fully edited and content may change prior to final publication. Citation information: DOI 10.1109/TOH.2023.3273908

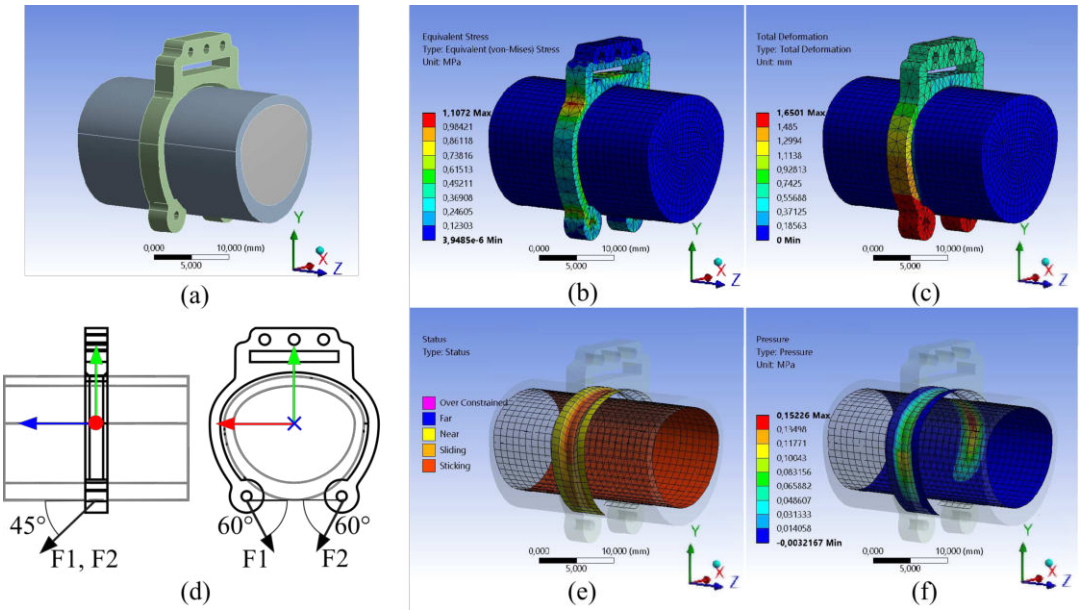

Fig. 5: Ring-phalanx model: a) CAD model of the ring-phalanx system, including the bone and the tissue; b) Equivalent (von-Mises) Stress; c) Total Deformation; d) model of application of the forces, in evidence the angles on the YZ and XY planes; e) Contact Status; f) Contact Pressure.

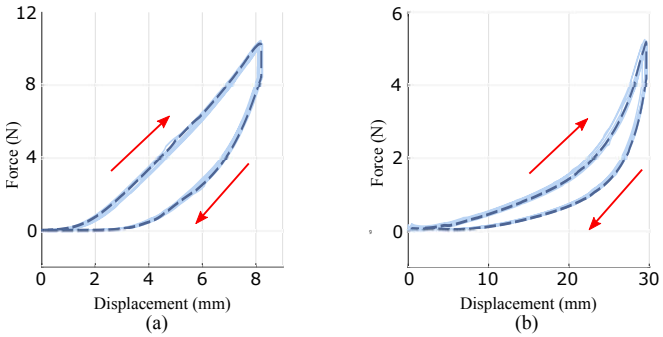

Fig. 6: Force-displacement curve in loading and unloading conditions: a) ring longitudinal configuration; b) ring lateral configuration. In red are the directions for loading and unloading.

about $20\,mm$. Figure 8 shows these data with respect to the time (a, b) and the relationship between the displacement of the two fingers and the force generated by the middle finger (c). The test evaluated also the robustness of the transmission in recovery from slack branches (i.e. the opening branch of the index finger in the test). Due to the depth of the grooves and the limited number of tendon turns in the pulley (approximately 2 turns), the transmission was safely recovered during all the repetitions in the experiment.

From the third test with FSR sensors, the hand-palm plate interface pressure was measured at three different voltage references. Figure 9 shows the measured pressure and the sensor placement under the glove. On the index side, the maximum pressure is $154\ mBar$ and, on the little finger side, it is $59\,mBarr$.

From the first characterization test of the exoskeleton with subjects, the relationship between the force applied by the motor and the force generated by the exoskeleton has been extracted. Figure 10 A shows the exoskeleton force as a function of the motor force. It shows an average ratio between the grasping force and the motor output force of 37%.

The force-displacement curve in loading conditions for the exoskeleton has been computed from the same experimental data (Figure 10b).

Figure 12a shows an example of measured pressure, averaged over ten trials. After a short movement in which the exoskeleton brings fingers into contact with the object, pressure increases until a plateau is reached.

Figure 12b shows the maximum measured grasping pressure reached for each subject, averaged over 10 repetitions. The maximum grasping pressure is in the range between $72\,mBar$ and $126\,mBar$. Pearson linear regression analysis showed a significant relationship between the maximum force and the hand length ($r^2 = 0.82$, $p < 0.05$).

As a qualitative report by healthy subjects, when asked whether the exoskeleton was comfortable during the experimental session, they reported no pain or fatigue was felt. It has to be considered the length of the characterization experimental session (about 30 minutes for each subject) was limited in time. However, they reported forces applied by tendons were highly perceivable especially along the axial finger direction and at the fingertips. This might suggest a possible limit to the tendon force concerning the comfort of the device.

Regarding the SCI patient, the exoskeleton generated a grasping pressure of $21\ mBar$, whereas the patient alone was capable of a maximum voluntary grasping pressure of $4\ mBar$ (results shown in Figure 13). Although the

This article has been accepted for publication in IEEE Transactions on Haptics. This is the author's version which has not been fully edited and content may change prior to final publication. Citation information: DOI 10.1109/TOH.2023.3273908

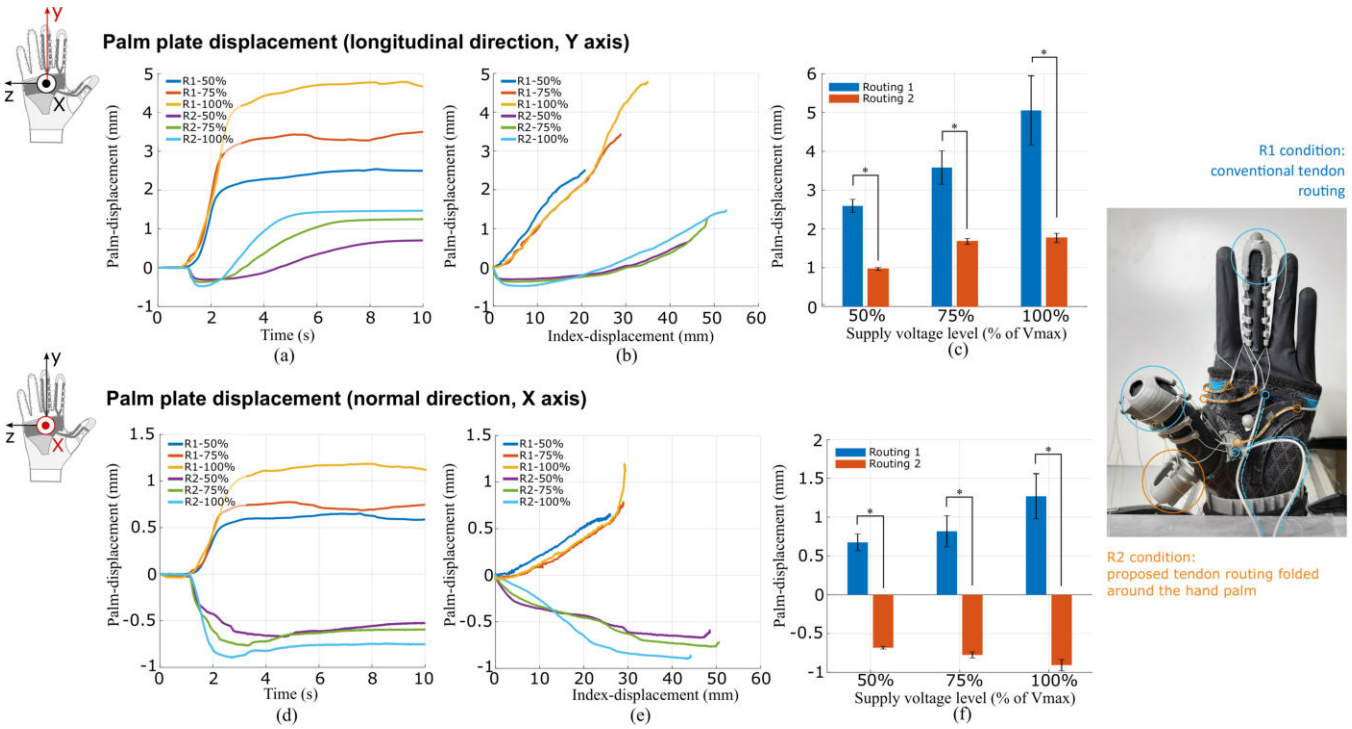

Fig. 7: Bench test measuring relative displacement of the device with respect to the hand when activated in the closing direction. (a,b,c) displacement in the longitudinal direction (Y); (d,e,f) displacement normal to the palm (X). R1 is the cable routing resembling conventional Bowden cable transmission. R2 is the proposed cable routing folded around the hand palm. The statistical significance between R1 and R2 conditions was assessed with a paired t-test ($\alpha = 0.05$). All the differences were statistically significant with a p-value less than 0.001. The device is worn by a hand mannequin.

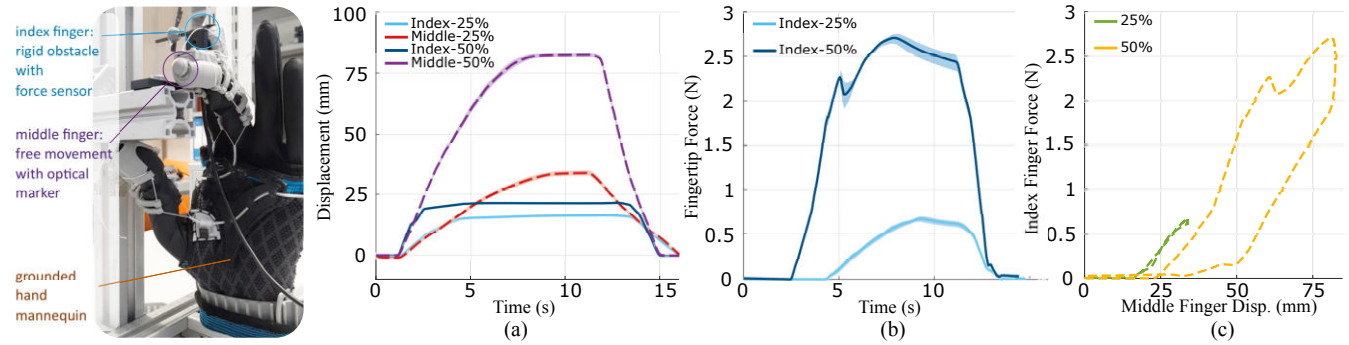

Fig. 8: Bench test measuring inter-finger compliance: (a) displacement of the markers on the index and middle fingertips, (b) measured force generated by the middle finger in contact with the fixed obstacle with the force sensor, (c) force generated by the middle finger, plotted with respect to the displacement of both fingers.

exoskeleton was able to significantly increase the closing force, a firm grasp of the object was impeded by the low friction generated between the object and the TPU parts of the soft exoskeleton. In comparison, we report a result we presented in [31]: there, a repeated grasping and lift task was performed by the experimenter using bare fingers and the same pressure sensorized bottle (total mass 0.5 Kg). The minimum pressure required to lift the bottle without slipping was $7.5\,mBar$.

IV. DISCUSSION

Regarding finger units, we adopted the solution proposed in [19], further characterizing the open-ring elements by simulation and experimental loading tests. The FEM simulation preliminary evaluated the deformation and stress of the open-ring structure under the expected loading condition and assessed a considerable safety margin with respect to tendon actuation forces. Moreover, the FEM simulation explored the distribution of pressure between the ring and finger tissues. Evaluation of the peak value provided indicative information of comfort and possible risks for the user: the maximum simulated pressure was well below the pain

This article has been accepted for publication in IEEE Transactions on Haptics. This is the author's version which has not been fully edited and content may change prior to final publication. Citation information: DOI 10.1109/TOH.2023.3273908

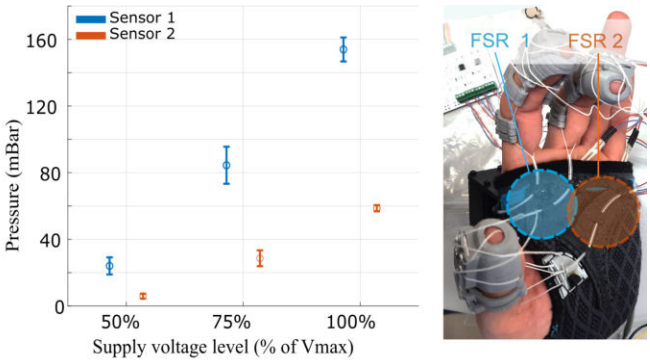

Fig. 9: Hand-palm plate interface pressure: (a) pressures at three different voltage references, (b) photo of sensor placement under the glove

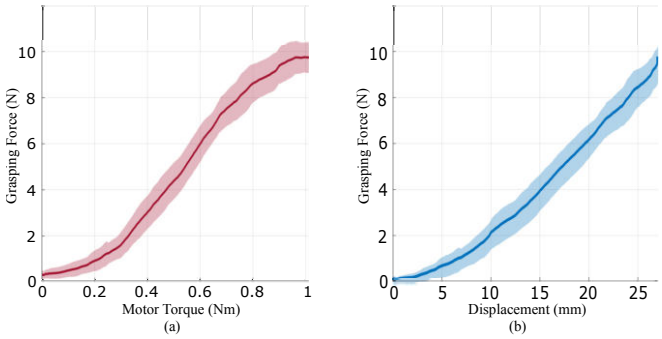

Fig. 10: Device characteristics from grasping experiment with healthy subjects: (a) grasping force vs. motor torque (dashed line with standard deviation area), (b) grasping force vs. cable displacement for the index finger closing transmission (dashed line with deviation area).

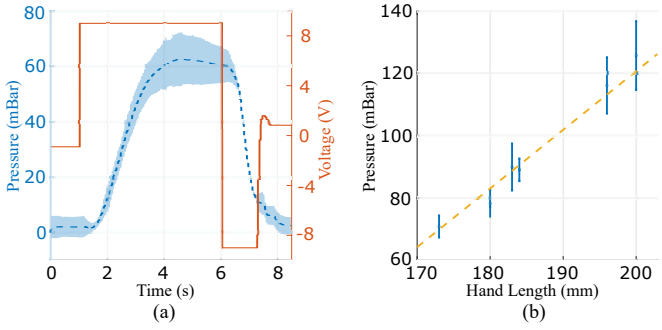

Fig. 11: Measured grasping pressure with healthy subjects: example of measured pressure vs applied voltage (a) and maximum pressure reached by each passive user (b), averaged over ten trials.

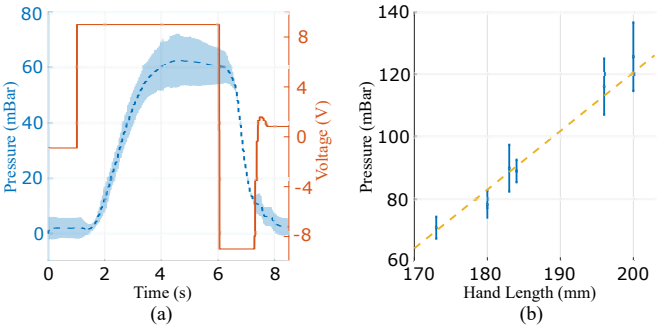

Fig. 12: Measured grasping pressure with healthy subjects: example of measured pressure vs applied voltage (a) and maximum pressure reached by each passive user (b), averaged over ten trials.

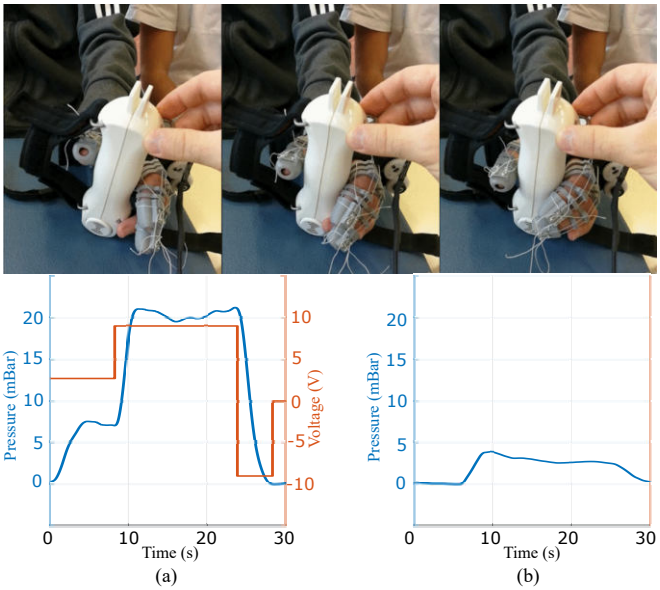

Fig. 13: (top) The assisted closing sequence of the SCI patient's hand. (bottom) Measured grasping pressure with SCI subject: (a) assisted by the exoskeleton; (b) without the exoskeleton.

threshold. This is a relevant point considering the high tendon forces typically needed in soft exoskeleton devices. Experimental characterization of the open ring compliance evaluated the desired different behavior in the lateral and vertical directions of loading. High flexibility in the lateral direction allows more comfortable adaptation to the finger, whereas stiffness in the vertical direction is required to withstand forces applied by the tendon transmission. The number of rings used in the experiments was chosen as a trade-off between the distribution of forces and the maximum hand closure allowed by the device. When the hand is fully closed, the lower tips of the rings might come in contact one each other, eventually limiting the maximum hand closure. We ensured for each subject that a full closure of the hand was allowed. The position and distribution of the rings were observed stable during the repeated closing-opening cycles of the experimental tests.

Regarding the proposed tendon routing, the performed experiments aimed at quantitatively measuring the improved stability of the solution. Measurements of deformation through optical markers showed a decreased slippage of the device along the hand when tendons are activated. Results were directly compared to a conventional tendon routing we arranged on the same prototype. The novel tendon routing applies additional clenching forces, stabilizing the wearing of the device, only when the grasping assistance is active. Also, the clenching effect avoids detachment of the tendons from the palm into the hand-closing workspace, hindering object grasping (with the proposed routing, displacement of tendons at the palm is instead negative in the normal direction). These forces are released when the hand is at rest, with expected improvements in terms of comfort for the user.

The experiment with FSR sensors was conducted to support comparisons of tendon routing. Since conventional routing has been shown to fail to maintain the grip on the palm of the hand and to detach the plate, this experiment was only conducted on our routing and we have evaluated how much pressure the plate exerted on the palm of the hand, which contributes to stability. The difference in pressure between the two sensors on the palm can be explained by the fact that on the index finger side two pairs of cables run, contributing to the clenching forces, while on the little finger side only one pair.

The experiment evaluating the inter-finger compliance was conducted to investigate the capability of the device to adapt to different grasping objects, given that the finger modules are not independently driven by the single multi-groove pulley. Results showed relevant inter-finger compliance, with a position difference between the constrained and the free-motion finger of 75 mm between fingertips (at maximum nominal load). The main compliance effect is expected to be introduced by the soft structure of the glove coupled with soft hand tissues, and by the stiffness of the tendons. At the given maximum loading force applied by the actuator, the deformation of each tendon is estimated equal to 23 mm. This behavior can cope with both grasping of non-cylindrical objects, and different finger proportions between users. Elasticity of the tendon transmission in multi-fingered robotic grasping resembles the concept of soft synergies, investigated here [32] to increase adaptability to the environment.

In the experiments with subjects, all subjects were able to wear the prototype and they verbally reported being comfortable wearing the device on the hand palm and on the fingers. However, when the transmission was loaded, most of the tension was reported to be perceived at the fingertips, evidencing the need for a different and more compliant design for the thimbles. Also, although the device showed a stable pose of the hand during grasping, firm grasping of the objects when lifted was compromised by the low friction presented by the soft material of the thimbles.

In terms of grasping capabilities, the exoskeleton was able to mobilize the passive hand, applying a considerable maximum grasping force and pressure ($12.8\ N$ and $118.4\ mBar$). The trend of the grasping pressure compared to hand size shows the exoskeleton performs better with bigger hands: although the geometrical factors determining this relationship need further investigation, the experiment provides information about limits in the adaptability of the actual prototype.

Compared to the literature, other proposed prototypes reached higher maximum grasping forces, still at the cost of noticeably higher loading force in the tendon transmission. Measurements of the exoskeleton grasping force and of the motor force showed an average ratio of 37% in the proposed prototype. This improves over similar tendon actuated devices, i.e. [22], [33] and [24] with an estimated ratio between grasping and tendon force ranging from 16% to 35%. The efficiency of the transmission is important to reduce forces applied to the user's hand. based on the qualitative comments of the healthy participants, we expect that in prolonged use, limits to the maximum grasping force might be imposed by the comfort of the user rather than by the dimensions of the actuators. Regarding the specific additional clenching forces at the hand palm, verbal reports from healthy subjects did not evidence uncomfortable perception or issues, whereas pulling forces at the fingertips were reported as highly perceivable. It has to be noted that in the proposed design, the clenching force is well distributed at the hand palm and dorsum by the semi-rigid plates of the glove.

The novel tendon routing, with the closing branches folded around the hand palm, provided the opportunity of embedding the actuator at the hand dorsum, with a single output shaft and a multi-groove pulley. Although the same proposed routing and glove structure can be implemented with remote actuators, we decided to explore the embedded-actuator solution: it simplifies device actuation transmission and, we expect, it can improve dexterity in a variety of tasks. In a remote-actuator implementation, multiple sheaths with limited flexibility would derive from the hand, possibly limiting or hindering wrist and upper arm mobility. On the other side, our solution adds mass and volume to the hand, hence diminishing dexterity in the manipulation of objects with closed handles or similar geometrical constraints. The advantages and disadvantages of the two design solutions need to be addressed by a feasibility study with structured manipulation tasks. Still, the novel transmission layout can be applied seamlessly to a Bowden cable transmission, with sheath insertion points at the hand dorsum.

The choice of using a single actuator and a single degree of freedom was made along with the embedded actuator solution, allowing for a compact and lightweight actuated device. It results in an under-actuated finger operation, with properties determined by the intrinsic compliance of the soft exoskeleton structure. The conducted experiments measuring inter-finger compliance showed the capability of the fingers to adapt to non-cylindrical grasping, although driven by a single actuator. These experiments indirectly tested also the robustness of the exoskeleton to loosen tendon transmission (in the extreme condition when one finger is blocked and the other closes, the opening tendon of the finger is loosened). We did not implement a specific anti-slack mechanism as in

[19]. To limit the encumbrance of the embedded actuator, we preferred to increase the depth of the grooves in the actuating pulley, obtaining robustness to tendon loosening in all the observed operative conditions.

The tests with SCI patients, although very preliminary, evidenced important aspects of the developed design.

The spasticity of the first patient, coupled with a small hand, impeded the operation of the device. The device performed well with the second SCI patient presenting a longer hand and almost no spasticity. The soft exoskeleton was able to mobilize the hand and provide evident support to the grasping force. However, the TPU material of the finger units did not show adequate friction to allow a firm grasp of the object. Different materials (i.e. silicone rubber) or coatings can be introduced for parts in contact with the grasped objects. It was also noted that the object was more prone to slip away from the hand than with healthy subjects: this might be due to a lack of support for holding the thumb in the correct pose, which might have been involuntarily compensated by the healthy subjects. The effect would explain the noticeably different maximum grasping pressure obtained between subjects and the patient.

The whole structure of the exoskeleton has been designed with certain design guidelines to improve wearability by impaired hands. A full-glove structure was avoided, preferring finger modules separated from the plates at the hand palm and at the dorsum. Also, the open-ring elements and an opening on the full side of the glove (on the side of the little finger) help to don by impaired hands. Still, the tendon connections between parts impose some constraints with respect to fully detachable modules. Similarly, the adjustable length of cables by screw terminals at the fingertip resulted in a precious and undeniable feature, still, it has to be improved with faster solutions, that can be easily used by a therapist or by an assisting person.

V. CONCLUSIONS

In this work, we have presented the design, development, and experimental evaluation of a soft and compliant hand exoskeleton designed for grasping assistance. The main novelty of the design consisted of a different tendon routing for the closing transmission, folded laterally on both sides of the hand, in order to add clenching forces when the exoskeleton is activated to assist grasping. The clenching effect improves the stability of the structure, decreasing the undesired slippage of the glove and the detaching of the tendons from the palm toward the hand workspace. These undesired effects are typically present in conventional soft hand exoskeleton designs and are further increased by the high tendon forces required during operation. In the proposed design these additional clenching forces are released when the hand is relaxed, resulting in improved comfort for the user. Experiments conducted with optical markers assessed the desired effect during the operation of the implemented prototype.

The novel tendon routing provided the opportunity of arranging the actuators directly at the hand dorsum, although the same proposed methods could be applied to a remote-actuator implementation. Different advantages and disadvantages of this solution have to be considered: it removes several semi-rigid sheaths connected to the hand, at the cost of increased mass and volume at the hand segment. In this work we explored the embedded actuator solution achieving a working prototype with limited mass ($124\ g$).

To improve comfort and adaptation to different hand sizes, modular and soft ring elements were designed for the finger segments. The functional design proposed in [19] was adopted here and further characterized: FEM and test-bench experiments evaluated structural properties of the open-rings, together with simulation of the exerted skin pressure in relation to comfort for the user.

Overall, the functionality of the prototype was promising. Its main advantages in terms of adaptability to different hands come along with good performance in terms of grasping assistance, in particular regarding the efficiency of the transmission (ratio between tendon force and final grasping force) which resulted in noticeably higher than state-of-the-art prototypes.

On the other side, experiments highlighted improvements required to become effective as an assistive robotic tool. Improvements include improved fingertip friction for firm grasping, and semi-rigid support for the thumb to guarantee an adequate grasping workspace in patients.

Together with compliance and adaptation, another envisaged potential of the developed design is its customization for each patient. The proposed design allows for fine customization of the glove: the palmar part can be easily fitted on a properly sized glove, whereas the number and the diameter of the finger rings can be tailored to the wearer. This level of customization paves the way for a highly comfortable assistive device. Further experiments involving SCI patients will aim at higher customization of the device for each patient, based on the modular and flexible design approach.

ACKNOWLEDGEMENTS

This work was supported by project RoboGYM PR19-RR-P2, funded by Italian INAIL, and by project TELOS (CUP J52F20001040002) funded by Tuscany Region, Italy, and with the co-financing of the European Union - FSE-REACT-EU, PON Research and Innovation 2014-2020 DM1062 / 2021.

REFERENCES

[1] L. Cappello, J. T. Meyer, K. C. Galloway, J. D. Peisner, R. Granberry, D. A. Wagner, S. Engelhardt, S. Paganoni, and C. J. Walsh, "Assisting hand function after spinal cord injury with a fabric-based soft robotic glove," *Journal of neuroengineering and rehabilitation*, vol. 15, no. 1, p. 59, 2018.

[2] Z. Lu, K.-y. Tong, H. Shin, A. Stampas, and P. Zhou, "Robotic hand–assisted training for spinal cord injury driven by myoelectric pattern recognition: A case report," *American Journal of Physical Medicine & Rehabilitation*, vol. 96, no. 10, pp. S146–S149, 2017.

[3] K. K. Ang, K. S. G. Chua, K. S. Phua, C. Wang, Z. Y. Chin, C. W. K. Kuah, W. Low, and C. Guan, "A randomized controlled trial of eeg-based motor imagery brain-computer interface robotic rehabilitation for stroke," *Clinical EEG and neuroscience*, vol. 46, no. 4, pp. 310–320, 2015.

[4] P. Heo, G. M. Gu, S.-j. Lee, K. Rhee, and J. Kim, "Current hand exoskeleton technologies for rehabilitation and assistive engineering," *International Journal of Precision Engineering and Manufacturing*, vol. 13, no. 5, pp. 807–824, 2012.

[5] M. Almenara, M. Cempini, C. Gómez, M. Cortese, C. Martín, J. Medina, N. Vitiello, and E. Opisso, "Usability test of a hand exoskeleton for activities of daily living: an example of user-centered design," *Disability and Rehabilitation: Assistive Technology*, vol. 12, no. 1, pp. 84–96, 2017.

[6] M. Cempini, M. Cortese, and N. Vitiello, "A powered finger–thumb wearable hand exoskeleton with self-aligning joint axes," *IEEE/ASME Transactions on mechatronics*, vol. 20, no. 2, pp. 705–716, 2014.

[7] D. Leonardis, M. Barsotti, C. Loconsole, M. Solazzi, M. Troncossi, C. Mazzotti, V. P. Castelli, C. Procopio, G. Lamola, C. Chisari, *et al.*, "An emg-controlled robotic hand exoskeleton for bilateral rehabilitation," *IEEE transactions on haptics*, vol. 8, no. 2, pp. 140–151, 2015.

[8] M. Sarac, M. Solazzi, D. Leonardis, E. Sotgiu, M. Bergamasco, and A. Frisoli, "Design of an underactuated hand exoskeleton with joint estimation," in *Advances in Italian Mechanism Science*. Springer, 2017, pp. 97–105.

[9] C.-Y. Chu and R. M. Patterson, "Soft robotic devices for hand rehabilitation and assistance: a narrative review," *Journal of neuroengineering and rehabilitation*, vol. 15, no. 1, p. 9, 2018.

[10] H. K. Yap, J. H. Lim, F. Nasrallah, and C.-H. Yeow, "Design and preliminary feasibility study of a soft robotic glove for hand function assistance in stroke survivors," *Frontiers in neuroscience*, vol. 11, p. 547, 2017.

[11] X. Cao, K. Ma, Z. Jiang, and F. Xu, "A soft robotic glove for hand rehabilitation using pneumatic actuators with jamming structure," in *2021 40th Chinese Control Conference (CCC)*. IEEE, 2021, pp. 4120–4125.

[12] A. Stilli, A. Cremoni, M. Bianchi, A. Ridolfi, F. Gerii, F. Vannetti, H. A. Wurdemann, B. Allotta, and K. Althoefer, "Airexglove—a novel pneumatic exoskeleton glove for adaptive hand rehabilitation in post-stroke patients," in *2018 IEEE international conference on soft robotics (RoboSoft)*. IEEE, 2018, pp. 579–584.

[13] Y. Jiang, D. Chen, P. Liu, X. Jiao, Z. Ping, Z. Xu, J. Li, and Y. Xu, "Fishbone-inspired soft robotic glove for hand rehabilitation with multi-degrees-of-freedom," in *2018 IEEE International Conference on Soft Robotics (RoboSoft)*. IEEE, 2018, pp. 394–399.

[14] N. Takahashi, S. Furuya, and H. Koike, "Soft exoskeleton glove with human anatomical architecture: production of dexterous finger movements and skillful piano performance," *IEEE Transactions on Haptics*, vol. 13, no. 4, pp. 679–690, 2020.

[15] T. Bützer, O. Lambercy, J. Arata, and R. Gassert, "Fully wearable actuated soft exoskeleton for grasping assistance in everyday activities," *Soft Robotics*, vol. 8, no. 2, pp. 128–143, 2021.

[16] V. Nazari, M. Pouladian, Y.-P. Zheng, and M. Alam, "A compact and lightweight rehabilitative exoskeleton to restore grasping functions for people with hand paralysis," *Sensors*, vol. 21, no. 20, 2021. [Online]. Available: https://www.mdpi.com/1424-8220/21/20/6900

[17] S. W. Lee, K. A. Landers, and H.-S. Park, "Development of a biomimetic hand exotendon device (biomhed) for restoration of functional hand movement post-stroke," *IEEE Transactions on Neural Systems and Rehabilitation Engineering*, vol. 22, no. 4, pp. 886–898, 2014.

[18] M. Xiloyannis, L. Galli, D. Chiaradia, A. Frisoli, F. Braghin, and L. Masia, "A soft tendon-driven robotic glove: Preliminary evaluation," in *International Conference on NeuroRehabilitation*. Springer, 2018, pp. 329–333.

[19] B. B. Kang, H. Choi, H. Lee, and K.-J. Cho, "Exo-glove poly ii: A polymer-based soft wearable robot for the hand with a tendon-driven actuation system," *Soft robotics*, vol. 6, no. 2, pp. 214–227, 2019.

[20] R. Alicea, M. Xiloyannis, D. Chiaradia, M. Barsotti, A. Frisoli, and L. Masia, "A soft, synergy-based robotic glove for grasping assistance," *Wearable Technologies*, vol. 2, 2021.

[21] D. H. Kim, Y. Lee, and H.-S. Park, "Bioinspired high-degrees of freedom soft robotic glove for restoring versatile and comfortable manipulation," *Soft Robotics*, 2021.

[22] H. In, B. B. Kang, M. Sin, and K.-J. Cho, "Exo-glove: A wearable robot for the hand with a soft tendon routing system," *IEEE Robotics & Automation Magazine*, vol. 22, no. 1, pp. 97–105, 2015.

[23] A. Ribas Neto, J. Fajardo, W. H. A. da Silva, M. K. Gomes, M. C. F. de Castro, E. Fujiwara, and E. Rohmer, "Design of tendon-actuated robotic glove integrated with optical fiber force myography sensor," *Automation*, vol. 2, no. 3, pp. 187–201, 2021.

[24] D. Popov, I. Gaponov, and J.-H. Ryu, "Portable exoskeleton glove with soft structure for hand assistance in activities of daily living," *IEEE/ASME Transactions on Mechatronics*, vol. 22, no. 2, pp. 865–875, 2016.

[25] T. Bagneschi, D. Leonardis, D. Chiaradia, and A. Frisoli, "A compact soft exoskeleton for haptic feedback in rehabilitation and for hand closing assistance," in *International Conference on NeuroRehabilitation*. Springer, 2020, pp. 629–633.

[26] "Internal morphology of human phalanges," *Journal of Hand Surgery*, vol. 9, pp. 490–495, 1984. [Online]. Available: http://dx.doi.org/10.1016/S0363-5023(84)80099-4

[27] A. Abdouni, M. Djaghloul, C. Thieulin, R. Vargiolu, C. Pailler-Mattei, and H. Zahouani, "Biophysical properties of the human finger for touch comprehension: Influences of ageing and gender," *Royal Society Open Science*, vol. 4, 2017.

[28] A. N. Natali and E. A. Meroi, "A review of the biomechanical properties of bone as a material," *Journal of Biomedical Engineering*, vol. 11, pp. 266–276, 1989.

[29] Gyrobot, "Flexy-hand," in *[online] Available: www.thingiverse.com/thing:242639*, 2014.

[30] J. Brennum, M. Kjeldsen, K. Jensen, and T. S. Jensen, "Measurements of human pressure-pain thresholds on fingers and toes," *Pain*, vol. 38, pp. 211–217, 8 1989.

[31] D. Leonardis and A. Frisoli, "Cora hand: a 3d printed robotic hand designed for robustness and compliance," *Meccanica*, vol. 55, no. 8, pp. 1623–1638, 2020.

[32] M. G. Catalano, G. Grioli, E. Farnioli, A. Serio, C. Piazza, and A. Bicchi, "Adaptive synergies for the design and control of the pisa/iit softhand," *The International Journal of Robotics Research*, vol. 33, no. 5, pp. 768–782, 2014.

[33] A. Yurkewich, I. J. Kozak, D. Hebert, R. H. Wang, and A. Mihailidis, "Hand extension robot orthosis (hero) grip glove: enabling independence amongst persons with severe hand impairments after stroke," *Journal of neuroengineering and rehabilitation*, vol. 17, no. 1, pp. 1–17, 2020.